EUROPEAN ORGANIZATION FOR NUCLEAR RESEARCH
European Laboratory for Particle Physics

Large Hadron Collider Project

LHC Project Report 888

Development of a Current Fit Function for NbTi to be Used for Calculation of Persistent Current Induced Field Errors in the LHC Main Dipoles

N. Schwerg, C. Vollinger

Abstract

A new fit function for the critical current density of superconducting NbTi cables for the LHC main dipoles is presented. Existing fit functions usually show a good matching of the very low field range, but produce a current density which is significantly too small for the intermediate and high field range. Consequently the multipole range measured at cold is only partially reproduced and loops from current cycling do not match. The presented function is used as input for the field quality calculation of a complete magnet cross-section including arbitrary current cycling and all hysteresis effects. This way allows to trace a so-called finger-print of the cable combination used in the LHC main bending magnets. The finger-print pattern is a consequence of the differences of the measured superconductor magnetization of cables from different manufacturers. The simulation results have been compared with measurements at cold obtained from LHC main dipoles and a very good agreement for low and intermediate field values could be observed.

CERN, Accelerator Technology Department, Geneva, Switzerland

Presented at the 19th International Conference on Magnet Technology (MT19)
18-23 September 2005, Genova, Italy

CERN
CH - 1211 Geneva 23
Switzerland

Geneva, 19 May 2006

Development of a Current Fit Function for NbTi to be Used for Calculation of Persistent Current Induced Field Errors in the LHC Main Dipoles

Nikolai Schwerg, Christine Vollinger

Abstract— **A new fit function for the critical current density of superconducting NbTi cables for the LHC main dipoles is presented. Existing fit functions usually show a good matching of the very low field range, but produce a current density which is significantly too small for the intermediate and high field range. Consequently the multipole range measured at cold is only partially reproduced and loops from current cycling do not match. The presented function is used as input for the field quality calculation of a complete magnet cross-section including arbitrary current cycling and all hysteresis effects.**
This way allows to trace a so-called finger-print of the cable combination used in the LHC main bending magnets. The finger-print pattern is a consequence of the differences of the measured superconductor magnetization of cables from different manufacturers. The simulation results have been compared with measurements at cold obtained from LHC main dipoles and a very good agreement for low and intermediate field values could be observed.

***Index Terms*—Accelerator magnets, critical current, superconductor magnetization, critical surface.**

I. Introduction

KNOWING THE DEPENDENCY of the critical current density J_c on temperature and on the magnetic field is the key issue in the calculation of magnetization effects. Different approaches exist in literature for the determination of a current fit function for NbTi cables in an empirical way: Fitting of individual branches for the magnetization data [1] or developing a current fit function suited for a few points or even a single J_c measurement [2], [3] to characterize the strand.
In this paper, we developed a single expression for the fit function of the critical current density that is valid over the whole operation range of a magnet. In addition, the function had to stay sufficiently flexible to independently adapt to different ranges of the magnetic field while a certain simplicity had to be kept for incorporating the fit into an existing magnetization model [4] for the magnet calculation. At the same time, the fit has to be precise enough to distinguish for even small differences in the measured magnetization and this for the complete operating range of the magnet.
Having found such a sensitive fit, it is possible to compare cables of the same type produced by different manufacturers in order to develop a "finger-print" pattern of the cable such that the difference in the magnetization measurement taken on these cables is visible in the field quality pattern of magnets wound from different cables.

Manuscript received September 7, 2005. All authors are with CERN. Corresponding author is C. Vollinger, email: Christine.Vollinger@cern.ch, phone: +41-227671062.

II. Measured Data and Existing Fits

A wide range of data was resulting from magnetization measurements taken at CERN [5] on cables for the LHC main dipoles of which only the down-ramp branch had been used as shown in Fig. 1. The value taken as cable magnetization is the average of the measured magnetizations of individual strands used in the cable. The coil of the LHC main dipole consists of a two layer cosine-θ design of a Rutherford type cable (shown in Fig. 5). The inner layer cable, denoted as 01 is produced by two firms coded B and E, whereas the outer layer cable, denoted as 02 is produced by five firms coded B, C, D, G, K. This way, a coil could consist of a 01B02D cable combination (note that not all combinations exist).
Of the compared fits, the best match was obtained from the following function, being a fit of a scaling power law type [2]:

$$f(B) = J_{ref} \cdot C_0 \frac{1}{B} \left(\frac{B}{B_{c2}(T)}\right)^{\alpha} \left(1 - \frac{B}{B_{c2}(T)}\right)^{\beta} \left(1 - \left(\frac{T}{T_{c0}}\right)^{n}\right)^{\gamma} \quad (1)$$

with C_0, α, β, γ, n as fitting parameters. C_0 is a linear constant and J_{ref} the reference critical current density, given at (5 T, 4.2 K) and set to 3 kA/m^2 for LHC cables. This fit has been applied to all data as starting point.

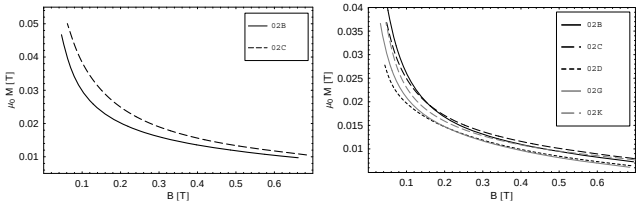

Fig. 1: Measured sc magnetization of the down-ramp branch for different cables. Data with courtesy of S. LeNaour [5].

However, it was soon obvious that the given parameter range had to be expanded vastly and especially β had to be set to much larger values than expected resulting in a change of the

physical behavior and giving the impression that a limit of the fit function has been reached. For β larger than 1, the term with β-dependency creates a parabola-like shape and causes a hysteresis width too small compared to measurements. In order to match the data, an adjustable bending behavior and the possibility to independently steer the high and low-field parts of the function without influencing the other was required. In addition, the fit function had to provide a higher critical current density in the intermediate field range (between 1 T and 5 T), if needed.

III. THE NEW FIT FUNCTION

A. Development of the Fit Function

1) Adjustable Bending Behavior

Part of the problem was that the measurement data covers the very low field range up to 800 mT only; we exploited the fact that the value for the critical field is a material property [6] and thus an additional extrapolation point can be added by scaling for the operating temperature to (13.5 T, 1.9 K) without considering the cable parameters that are resulting from engineering details of the cable (as, *e.g.* degree of cold working, shaping a Rutherford type cable etc.).

The magnetization data M(A/m) has been transformed into a curve for the critical current density on which the fit has been tried by*:* M=-4/3$\pi J_c r_f$ where r_f is the filament radius and the critical current density J_c(A/m^2) refers to the superconducting surface. Since the measurement data was limited to the low field range with only one added extrapolation point for high fields, it was necessary to strictly split the fit function into low, intermediate and high field parts with no or only little coupling between the low and high-field range and to provide an adjustable bending behavior. In addition, two slopes are distinguishable in the magnetization measurements which can be accounted for by multiplicative terms. Thus the function modeling the low field range reads:

$$f^*(B) = (a\,\mathrm{e}^{-Bb}+1)(c\,\mathrm{e}^{-Bd}+1)$$

and replaces $1/B(B/B_{c2}(T))^{\alpha}$ in the power law fit (PLF), eq.(1). This way, we get a double bending fit function (denoted DBF):

$$f(B) = J_{ref}\cdot C_0\cdot(a\,\mathrm{e}^{-Bb}+1)(c\,\mathrm{e}^{-Bd}+1)\,(1-\frac{B}{B_{c2}(T)})^{1.3}(1-(\frac{T}{T_{c0}})^n)^{\gamma} \quad (2)$$

with C_0, a, b, c, d as fitting parameters. Temperature dependency has not been considered but could be taken into account with the values taken from [2] where n=1.7 and γ=2.32 as long as the variation is small. C_0 is used as a linear parameter and J_{ref} is kept as in eq. (1). For high field values, the term $(1-B/B_{c2}(T))^{1.3}$ gets dominant and creates a function pinch-off in a similar way as it can be produced with the power law fit. Note, that the value of β, formerly being a fitting parameter with a given range of 0.64 to 1.1, could be fixed at 1.3 for all cable fits without deteriorating the result.

2) Range of the Fitting Parameters

The flexibility of the fit function with respect to the range of the fitting parameters is shown in Fig. 2. The fitting parameter a determines the slope of the function in the low field range and b is setting the bend and the rising point of the function. The combination results in a function with two curvatures, to be steered independently and with different bending points. Fig. 3 (left) shows the function with the lesser curvature (cont. line) rising smoothly into the steep low field part (dashed line). Adding the pinch-off term for the high field gives the final shape (right).

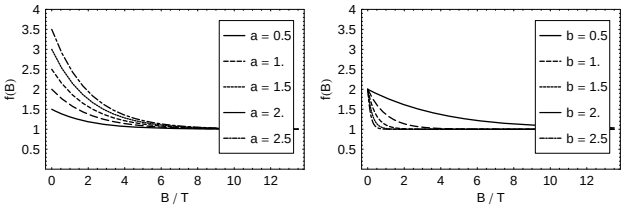

Fig. 2: Range of the fitting parameters a, b and decoupled steering.

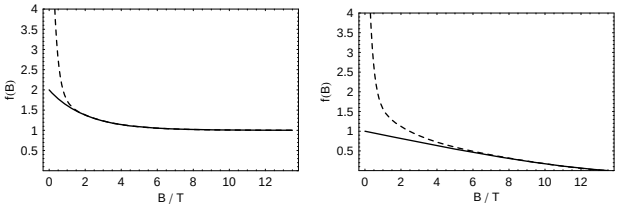

Fig. 3: Combination of curves with two slopes (left) and the pinch-off (right).

B. Applying the Fit Function to Magnet Calculation

1) Cable combinations

The coil of the LHC main dipole consists of a two layer cosine-θ design of (see Fig. 5, right). During production, the coil cross-section has been modified twice so that now three different coil cross-sections exist, of which the most of the magnets is produced with cross-sections 2 and 3.

Table I contains a summary of the fitting parameters obtained for each cable data set shown in Fig. 1. One can see that the fitting parameters C_0, a, b, c, d stay in the same range for all cables which is an indication that the fit is stable, except for cable 02D for which the fitting parameter d is considerably larger than for the other cables. The high value of d for cable 02D is to be expected from the measurement curves since the function bends at a lower field value than the others. For comparison we calculated the deviation as:

$$\chi^2 = \sqrt{\frac{1}{N}\sum_{n=1}^{N}(y_n - f(x_n))^2}$$

where (x_n, y_n) is one pair of measurement data and $f(x_n)$ the value of the fit function in the respective position.

TABLE I
PARAMETERS AND STANDARD DEVIATION FOR THE NEW FIT FUNCTION

	01B	01E	02B	02C	02D	02G	02K
C0	4.29	4.506	4.077	4.518	3.941	3.215	4.480
a	3.0	3.30	3.40	3.20	3.55	4.5	2.95
b/T	3.20	3.0	3.0	3.0	3.50	3.20	3.15
c	1.725	1.414	1.991	1.479	1.063	1.403	2.000
d/T	19.87	12.55	17.90	18.80	32.62	25.36	23.37
$\chi^2\cdot10^3$/T	0.094	0.091	0.083	0.075	0.083	0.065	0.095

2) Evaluation and comparison with other fit functions

With the parameter pairs (*a,b*) and (*c,d*), the two slopes of the magnetization function can be adapted independently. Fig. 4 shows the matching of the curves to the J_c-function converted from the measured magnetization in the range of (0, 2 T) (left) and the normalized difference between measurement and fit (right). For comparison, we added the results of the fit in eq.(1) to the plots and gave the fitting parameters in Table II. These fitting parameters are in most cases out of the specified ranges given by the author, however, no satisfying fit could be found for the measured magnetization data for some of the cables when the function had been applied **and** the parameters were not allowed to leave their indicated range. This feature has already been observed by P.Gislon *et al*. at ENEA when applying the power law fit function to an NbTi strand [3].

TABLE II
PARAMETERS AND STANDARD DEVIATION FOR THE POWER LAW FIT FUNCTION

	01B	01E	02B	02C	02D	02G	02K
α	0.455	0.412	0.408	0.5	0.69	0.586	0.462
β	2.015	3.481	2.308	3.464	11.7	9.671	1.077
C0/T	15.86	16.55	14.22	21.61	46.26	29.33	16.45
$\chi^2 \cdot 10^3$/T	0.146	0.165	0.151	0.090	0.086	0.164	0.207

Cables 02D and 02G are shown only, of which 02G gives the best agreement, and 02D is considered as typical result for the new fit function.

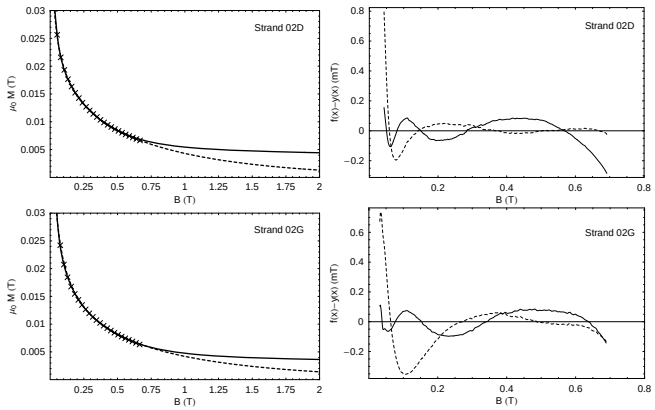

Fig. 4: Left: Matching of measurement data and fit function for a range of (0, 2 T) for different cables; dots: measurement, continuous line: new fit function, dashed line: Power law fit. Right: Absolute difference between measurement and the two fit curves for the low field range; continuous line: new fit function, dashed line: Power law fit (PLF).

We have plotted in Fig. 4 (right) the absolute difference between the measurement and the two fit curves for the low field range. It can be seen from the curves that a good agreement with the magnetization measurement can be found with both fit functions for the low field range below 0.8 T, of which also measurement data existed. However, in the intermediate range (starting **above** 1 T), the values for the magnetization resulting from the power law fit function prove to be too low (plots on the left of Fig. 4). Thus, also the critical current density used for the field error calculation is too small and the hysteresis widths of the multipoles (shown in Table III) do not reproduce the measurement. The same problem is observed in the high field range above 5 T (not shown in the plots).

3) Numerical calculation

The current fit has been used as input for the magnetization model [4] for the calculation of persistent currents by means of the ROXIE program [7]. Two sets of fitting parameters according to the inner and outer layer cable have been fed and an LHC dipole cross-section has been calculated.

The validity of the fit can be verified either by comparison with the measured magnetization data or, more complex, by applying the fit function to an existing magnet design and comparing the resulting multipoles with measurements taken at cold. After having tested the fit on the magnetization data, the approach of comparing with magnetic measurements taken at cold has been chosen for some magnets since no magnetization data exists for the intermediate and high field range.

From the calculation, it can be observed that general statements that persistent currents are affecting field quality in a magnet for the very low range only are misleading, since the field quality depends on the local distribution of the overall field within the coil cross-section comprising low field areas as well. These low field areas influence field quality in the intermediate range significantly, as it has already been shown in [8] even if they are located in the outer layer of the coil, as was the case for our geometry. To demonstrate this, we compared the calculation results for the hysteresis width at injection field level and in the intermediate field range from different cable combinations when the two fit functions are applied. Table III shows the simulation results and the values measured at cold.

TABLE III
CALCULATION AND MEASURED RESULTS OF THE HYSTERESIS WIDTH (IN UNITS) FOR TWO TYPICAL CROSS-SECTIONS AND RESPECTIVE CABLE COMBINATIONS

	X-section2 (01B02K)				X-section3 (01B02G)			
Magnet	3043 (meas)	3041 (meas)	DBF	PLF	3090 (meas)	3122 (meas)	DBF	PLF
at 760A	15.03	14.65	15.03	14.99	15.26	15.10	14.32	14.27
at 4kA	1.33	1.33	1.42	1.07	1.36	1.33	1.30	0.73

It can be seen from the values in Table III that both fit functions well reproduce the hysteresis widths in the low field range (around injection field level at 760 A), independent of the coil cross-section and the used cable. For the intermediate field range, the calculation results for the hysteresis width is too small and does not agree with the measurements taken at 1.9 K when the power law function (PLF) is applied, whereas values are very well reproduced with the double bending fit function (DBF). The calculation of a precise hysteresis width is needed, e.g., for the determination of the overall magnet losses of which hysteresis losses are the greatest part.

IV. IDENTIFYING A CABLE FINGER-PRINT

We used the results from the new fit function for the development of an identifying finger-print pattern of the cable to be visible in the field quality of a magnet that is wound from a certain cable combination. We could see that the hysteresis widths of the multipoles show a significant and systematic difference for multipoles of order 4 and higher depending on

the inner layer cable 01B and 01E. The largest effect is on the normal multipoles b5 and b7 (see Table IV), whereas no pattern is observed when different outer layer cables are used.

TABLE IV
HYSTERESIS WIDTH DEPENDING ON THE CABLE COMBINATION

01B					
	02B	02C	02D	02G	02K
Db3	15.26	15.59	14.27	14.31	15.02
Db5	-1.57	-1.59	-1.57	-1.58	-1.60
Db7	0.63	0.63	0.65	0.65	0.63

01E					
	02B	02C	02D	02G	02K
Db3	15.78	16.11	14.80	14.84	15.54
Db5	-1.83	-1.85	-1.82	-1.83	-1.85
Db7	0.74	0.73	0.75	0.75	0.74

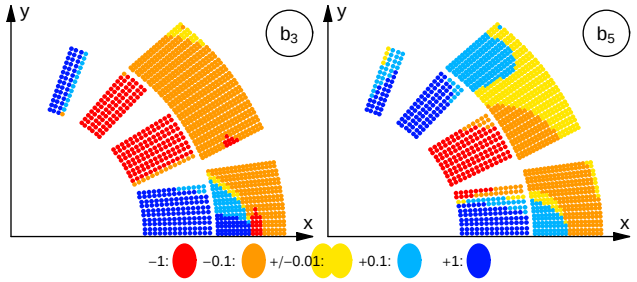

Fig. 5: First quadrant of the LHC main dipole coil cross-section with color coding of the contribution to the total field error for multipole b3 (left) and multipole b5 (right) showing that the contribution of the inner layer cable to b3 almost completely cancels out.

For multipole b3, contrary to expectations, little influence of the inner layer cable is observed since the coil geometry of the inner layer is such that the resulting magnetization contribution cancels out and the field error can be related almost completely to the outer layer cable. We have illustrated this by plotting field maps for the multipoles b3 and b5 in the first quadrant of the coil at injection field of 760 A (Fig. 5). The maps show in color coding the contribution of the individual strand to the respective field error normalized to the max. value. It can be seen that **individual** strands from the inner layer contribute more to the field error in both cases (b3 and b5), however, due to the sign change, the error on b3 cancels almost completely out for the inner **layer**, whereas on the outer layer, though the contribution is smaller, no cancellation takes place. From this, we calculated the ratio of the contribution of the layers and normalized it to the inner layer values, since it has been expected that the inner layer would dominate the field error. However, compared to the inner layer, the outer layer is the dominant part by contributing a field error 2.4 times higher for multipole b3. For multipole b5, we calculate a contribution to the total error of only 0.3 coming from the outer layer compared to the inner, thus showing an almost negligible contribution. All multipoles are shown in Table V. From the results in Table IV, we are able to identify the cable manufacturer of the inner layer cable from the hysteresis width of any multipole of order higher than 3. The outer layer cable manufacturer can be narrowed down in a second step from the hysteresis width of multipole b3, but cannot be uniquely identified due to the similarity of the cable magnetization of the outer layer cable.

TABLE V
RATIO OF THE MULTIPOLE CONTRIBUTION FOR THE OUTER LAYER W.R.T THE INNER LAYER DUE TO SUPERCONDUCTOR MAGNETIZATION

B1	b2	b3	b4	b5	b6	b7	b8	b9
0.83	4.74	2.35	1.70	0.29	0.07	0.05	0.05	0.02

V. CONCLUSION

We presented a fit function to be used as input for field quality calculation for NbTi cables with a high flexibility that reproduces the magnetization of the strand measured as well as the multipole errors measured in the LHC main dipoles at cold.

Since the measured magnetization values show a curve with two independent slopes, we showed that this shape can best be reproduced by means of combining two terms to be steered independently within one closed expression for the fit function. This is especially true if a large number of measurement points exist and/or if the data does not well cover the whole range of interest. Consequently, for detailed modeling, five fitting parameters seem to be justified. Comparison with cold data and calculations carried out with other fit functions support this statement.

VI. ACKNOWLEDGMENTS

We thank S. Sanfilippo, CERN, for the data from the magnetic measurements at 1.9 K and S. Le Naour, CERN, for providing the magnetization data.

REFERENCES

[1] R. Wolf, “Persistent Currents in LHC magnets”, IEEE Trans. Magn., vol.28, no.1, 1992.
[2] L. Bottura, “A Practical Fit for the Critical Surface of NbTi”, MT-16 Conference, Ponte Vendra Beach, USA, 1999.
[3] P. Gislon, *et al.*, “Electrical Characterization of the NbTi Strand for the ENEA Stability SEx-Up Experiment”, IEEE Trans. Appl. Supercond., vol. 13, no.2, 2003.
[4] M. Aleksa, *et al.*, “A Vector Hysteresis Model for Superconducting Filament Magnetization in Accelerator Magnets”, 14th COMPUMAG, Saratoga Springs, USA, 2003.
[5] S. Amet, *et al.*, “Persistent and Coupling Current Effects in the LHC Superconducting Dipoles”, Appl. Superc. Conf., Houston, USA, 2002.
[6] M.S. Lubell, “Empirical Scaling Formulas for Critical Current and Critical Field for Commercial NbTi”, IEEE Trans. Magn., no.3, 1983.
[7] S. Russenschuck, “Electromagnetic Design and Mathematical Optimization Methods in Magnet Technology”, ISBN: 92-9083-242-8.
[8] B. Bellesia, *et al.*, “Trends in Cable Magnetization and Persistent Currents during the Production of the Main Dipoles of the Large Hadron Collider”, Applied Supercon. Conference, Jacksonville, USA, 2004.